



# Fabrication, Microstructure, Hardness and Magnetic Properties of (W:Ti)C-Ni Cemented Carbides using Atomized Ni Powder

By Amal. A. Abd-Elghany, Walid M. Daoush, Omayma A. El-Kady,  
Mohamed A. Ghanem & Ahmed E. El-Nikhaily

*Helwan University*

**Abstract-** (W:Ti)C cemented carbides with different Ni content fabricated by powder metallurgy technique were investigated. The Ni powder which used as a metal binder of the (W:Ti)C-Ni abrasive particles was fabricated by water atomization technique by means of induction furnace. A Ni powder of a cubical particle shape with average particle size of 2-20  $\mu\text{m}$  was obtained. Six (W:Ti)C-Ni compositions with Ni contents of 5, 10, 15, 20, 25 and 30 wt.% were prepared by mechanical milling of the obtained atomized Ni powder with the abrasive (W:Ti)C particles followed by cold compaction at 600 MPa and vacuum sintering at 1450oC. Dense (W:Ti)C-Ni cemented carbides were obtained with a relative density of up to 94% with 30 wt% Ni.

**Keywords:** *water atomization; sintering, (W:Ti)C-Ni cemented carbides; hardness; magnetic properties.*

**GJRE-G Classification:** FOR Code: 290502



*Strictly as per the compliance and regulations of:*



# Fabrication, Microstructure, Hardness and Magnetic Properties of (W:Ti)C-Ni Cemented Carbides using Atomized Ni Powder

Amal. A. Abd-Elghany<sup>α</sup>, Walid M. Daoush<sup>σ</sup>, Omayma A. El-Kady<sup>ρ</sup>, Mohamed A. Ghanem<sup>ω</sup>  
& Ahmed E. El-Nikhaily<sup>¥</sup>

**Abstract-** (W:Ti)C cemented carbides with different Ni content fabricated by powder metallurgy technique were investigated. The Ni powder which used as a metal binder of the (W:Ti)C-Ni abrasive particles was fabricated by water atomization technique by means of induction furnace. A Ni powder of a cubical particle shape with average particle size of 2-20 μm was obtained. Six (W:Ti)C-Ni compositions with Ni contents of 5, 10, 15, 20, 25 and 30 wt.% were prepared by mechanical milling of the obtained atomized Ni powder with the abrasive (W:Ti)C particles followed by cold compaction at 600 MPa and vacuum sintering at 1450°C. Dense (W:Ti)C-Ni cemented carbides were obtained with a relative density of up to 94% with 30 wt% Ni. The hardness of the dense (W:Ti)C-30 wt.%Ni was greater than the hardness of other different compositions; The magnetic properties, which were measured at an applied field of 2tesla, indicate that the (W:Ti)C-Ni cemented carbides have ferromagnetic properties with a higher mass saturation magnetization with higher nickel content.

**Keywords:** water atomization; sintering, (W:Ti)C-Ni cemented carbides; hardness; magnetic properties.

## 1. INTRODUCTION

Cemented carbides are used as oxygen-free ceramics in high temperature engineering applications due to its properties like, high melting temperature, hardness, elastic moduli, wear resistance, electric conductivity and high-temperature strength. Cemented carbides are also widely applied as a base of hard metals. Applications of cemented carbides include structural, heating and reflecting functions as well as tool materials in composition with other refractory compounds [1]. The compacted products of these compounds are made by powder metallurgy technology where sintering methods are of decisive importance.

In General; cemented carbides are composite materials, which consist of hard refractory carbides

containing metals of the transition groups IV, V and VI (such as WC, TiC, TaC, NbC) embedded in a tough metal binder phase like nickel or cobalt which are by far the dominating binder metals employed due to its excellent wetting to WC and its good thermo-mechanical properties [2-4].

(W,Ti)C has a high melting point and high hardness than the commercial WC. In this regard, the transition metal carbide is primarily used in cutting tools and as an abrasive material as a single phase or in composite structures. In the case of cemented (W,Ti)C, Co or Ni is added as a binder for the formation of composite structures[5-9].

There are two basic ways of obtaining cemented carbide: through melt-solidification processing at about 2000-2500 °C or by powder metallurgy processing at a temperature range of 1350-1500 °C. Fabrications of WC as well as TiC in metal-base alloys have been studied from both theoretical and practical points of view. However, the production of (W:Ti)C in metal matrices has received little attention. The comparatively light TiC particles may float during the preparation by conventional melting and casting route. A large difference in density between TiC and the metal matrix melt-results segregation in metal ingot. The (W:Ti)C as reinforcements innickel, cobalt and iron alloy melts may be more appropriate because its density(6.66 g/cm<sup>3</sup> for (Ti<sub>0.75</sub>:W<sub>0.25</sub>)C [10] and 9.1 g/cm<sup>3</sup> for (Ti<sub>0.5</sub>:W<sub>0.5</sub>)C [11]) is higher than that of TiC (4.25 g/cm<sup>3</sup>) and close to that of iron melt(7.8 g/cm<sup>3</sup>). The hardness of (Ti<sub>1-x</sub>:W<sub>x</sub>)C (19-21 GPa) [12] is more or less the same as that of TiC (18-23 GPa) [13]. However, the fracture toughness of (Ti<sub>1-x</sub>:W<sub>x</sub>)C (6.4-7.7 MPa m<sup>1/2</sup>) [14] is higher than that of TiC (3.5-4.3 MPa m<sup>1/2</sup>) [15, 16] and this may result better mechanical properties of the (Ti<sub>1-x</sub>:W<sub>x</sub>)C-reinforced composite compared to those of the TiC-reinforced composite.

The sintering step in the powder metallurgy process is the main determine step among the forming processes. It can be evaluated by measuring the mechanical properties like hardness and physical properties like density and magnetic properties of the sintered product. Magnetic data shows some interesting relations between the physical properties, such as

*Author α:* Department of Production Technology, Faculty of Industrial Education, Helwan University, Cairo, Egypt.

*e-mails:* wmdaoush@imamu.edu.sa, waliddaoush@outlook.com

*Author ρ:* Department of Chemistry, College of Science, Al Imam Mohammad Ibn Saud Islamic University, Al Riyadh, KSA.

*Author ω:* Powder Technology Division, Central Metallurgical R&D Institute (CMRDI), P.O. Box 87 Helwan, Cairo, Egypt.

*Author ¥:* Department of Mechanical Engineering, Faculty of Industrial Education, Suez University, Suez, Egypt.



relations between the physical properties, such as density, and the mechanical properties such as hardness. There is interdependence between the mass saturation magnetization,  $M_s$ , and the coercive force,  $H_c$ , both of which frequently occur in an inverse relation.  $M_s$  is mostly related to the amount of magnetic material present, whereas  $H_c$  appears to be strongly influenced by the interaction between the particles and the density or between the porosity and the grain size of the carbide phase [17, 18].

In this work, cold compaction and vacuum sintering of (W:Ti)C cemented carbides samples with different binder content of a homemade water atomized Ni powder were occurred. The densification and properties of the prepared cemented carbide samples were characterized by microstructure investigations based on measurements of magnetic and mechanical properties.

## II. EXPERIMENTAL

Elemental powder of Ni was prepared by atomization technique. Nickel powder was prepared by induction melting in graphite crucibles in air by superheated up to 1700°C and bottom pouring through a ceramic melt delivery nozzle of 6 mm diameter into a confined water atomizer operating at a pressure of 20 MPa. The high-pressure water jets were directed against the molten stream. The melt flow rate, estimated from the operating time and weight of the atomized melt, was about 4 kg/min. The water flow rate, calculated from the water consumption rate, was about 200 l/min. Table 1 list the atomization conditions adapted for Ni powder fabrication process. The size distribution of the Ni powder particles was measured by conventional mechanical sieving, and sieved powders with a specific size range of 20  $\mu\text{m}$  and 1  $\mu\text{m}$  were chosen for this investigation.

Table 1: Water atomization parameters adapted for Ni powder fabrication process.

Parameter	Condition
Pouring temperature, °C	1700
Nozzle angle	35°
Nozzle diameter, mm	6
Number of water jets	4
Molten stream flow rate, kg/min.	4
Water pressure, MPa	20
Water flow rate, l/min.	200
Water velocity, m/s	90

(W:Ti)C powder with a particle size ranged from 2-20 $\mu\text{m}$  with WC: TiC ratio of 1:1 was supplied from HC. Starck Co., Germany.

The produced atomized Ni and (W:Ti)C powders were used to prepare six samples with compositions of 5 wt.%, 10 wt.%, 15 wt.%, 20 wt.%, 25 wt.%, and 30 wt.% of a Ni binder mixed with (W:Ti)C by means of Agate mortar for 30 min. After the different

compositions were prepared, they under went cold compaction at 600 MPa in a uniaxial hydraulic pressing machine, where they were compressed into a cylindrical shape.

The cold compacts were sintered in a vacuum furnace at 10<sup>-3</sup>torr with graphite heating elements and at a heating rate of 5 °C/min in accordance with the sintering cycle shown in Fig1. The samples were heated at 120 °C for 2 h to dry any moisture content, and the temperature was then raised to 750 °C for one hour to expel any gases embedded in the pores. The temperature was raised again to 1450 °C for one hour to start the sintering process. Finally, the furnace was turned off and the sintered compacts were cooled for 8 h by means of a water cooling system.

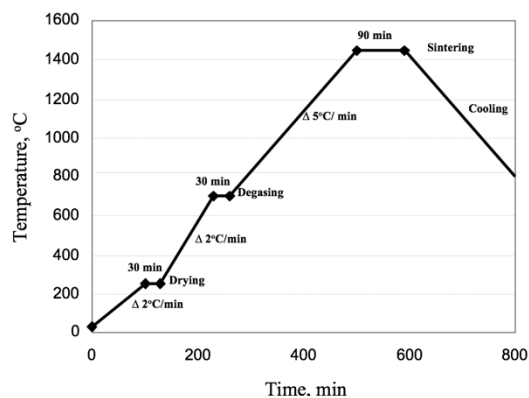


Figure 1: Heating cycle for the vacuum sintering process of (W:Ti)C–Ni cemented carbides at 1450 °C.

The dimensions of the cold compacts were measured before and after sintering to calculate the green, the sintered and the relative densities. The sintered samples were mounted and ground with 800, 1000, and 1200 grit SiC paper, respectively, and then polished with 3  $\mu\text{m}$  diamond paste. To investigate the microstructure of each phase as well as the compositional analysis of the carbide and liquid phase binder, scanning electron microscope (SEM, model: JEOL, JSM-5410) is used to take SEM micrographs and EDAX-SEM were used. The phases in the specimens were analyzed by means of X-ray diffraction (XRD), for which purpose we used a Cu Ka source and a x-ray diffract meter of the model x:pert PRO PAN analytical with Cu k $\alpha$  radiation ( $\lambda=0.15406\text{nm}$ ) diffract meter. The magnetic properties of samples were measured using vibrating sample magnetometer (model DEAS/FDD-2) in which the samples were vibrated at a constant frequency between a set of sense coils. As the magnetic field is varied through a specified range up to 2 Tesla, the magnetic moment of the sample is measured by the sense coils with a lock-in amplifier. The dependency between the magnetization and magnetic field (hysteresis loop) for the prepared samples was measured. Because the saturation magnetization changes with weight of the sample, the results were

divided by sample's weight. The magnetization values were expressed using the magnetic moment per gram (emu/g). The measured properties included saturation magnetization ( $M_s$ ), coercivity ( $H_c$ ) and remnant magnetization ( $M_r$ ). The hardness was measured with a Vickers hardness tester of the model Indentec 5030 SKG. The load was selected at 30 kgf. The test was repeated five times at different points in each sample, the average being reported.

### III. RESULTS AND DISCUSSION

Fig. 2(a) shows the typical SEM morphology of the as received (W:Ti)C powder. The particle shape of the as received powders was mostly irregular and had a rough surface morphology. Fig. 2(b) shows the typical optical morphology of the as atomized Ni powder. The particle shape of the as-solidified powders was mostly cubic to irregular and had a rough surface morphology. Fig. 2(c, d) shows the typical optical morphology of the admixed powder.

XRD analysis of the produced atomized Ni powder, as received (W:Ti)C as well as the admixed (W:Ti)C-Ni are shown in Fig. 3. It was observed from the results that the produced atomized Ni powder as well as the (W:Ti)C were composed only of its constituents without any foreign inclusions. On the other hand the admixed (W:Ti)C-Ni contains only the elemental constituents of the used powders. Fig. 4 shows the XRD pattern of the sintered (W:Ti)C-Ni composite at 1450°C by vacuum sintering. The results indicate the presence of (W:Ti)C and Ni in the sintered cemented carbides, meaning that the presence of a solid solution between WC and TiC at 1450°C. This is in good agreement with the equilibrium WC-TiC binary phase diagram [19]. Since there is almost no Ti solubility predicted in WC up to 2000°C, (W:Ti)C is close to pure WC and (Ti<sub>0.55</sub>W<sub>0.45</sub>)C in composition.

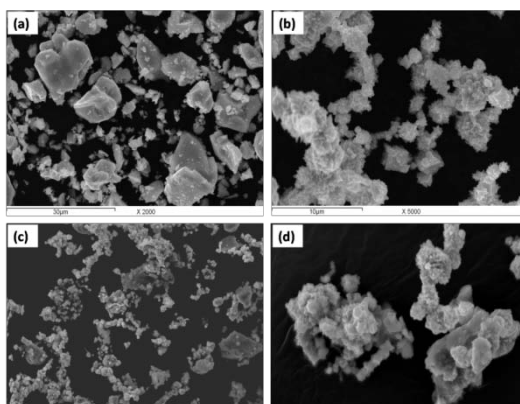


Figure 2: SEM Images for the investigated powders; where a) as received (W:Ti)C, b) the prepared atomized Ni

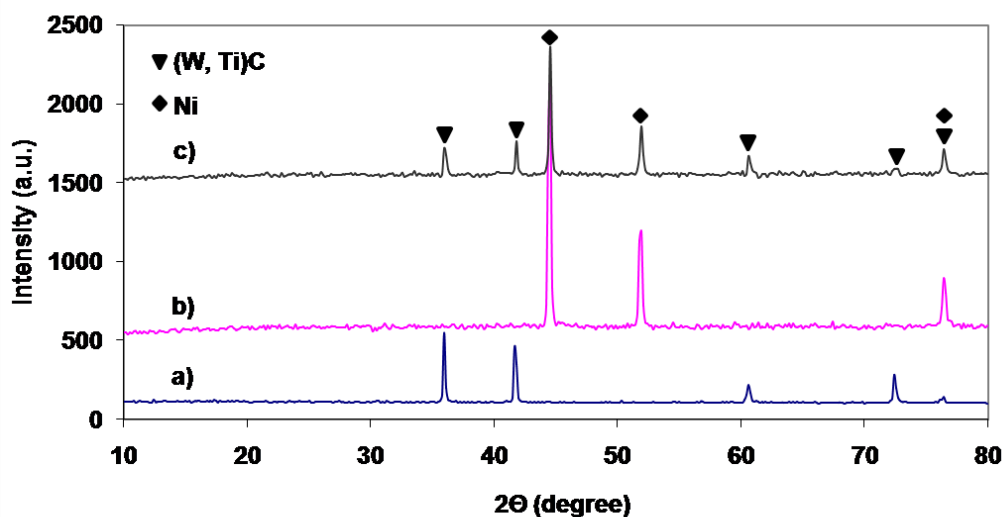


Figure 3: XRD pattern for the investigated powders, where: (a) as received (W,Ti)C, (b) atomized Ni and (c) admixed (W:Ti)C-30wt%Ni.

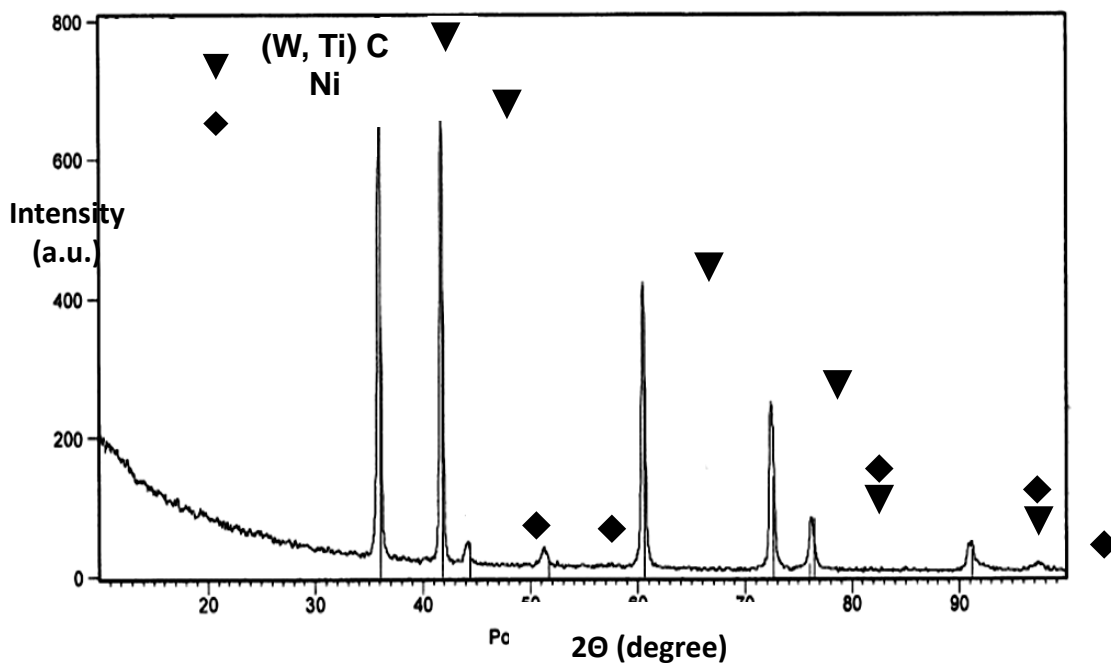


Figure 4: XRD pattern for the produced (W:Ti)C-20wt%Ni cemented carbide by vacuum sintering at 1450°C for 1h.

The maximum attainable densification of the obtained (W:Ti)C-Ni cemented carbides are due to the particles rearrangement is influenced by different parameters, such as the amount of liquid present, the particle size, the contact angle, and the solubility of the solid in the liquid. Fig.5 shows the results of the micro structural investigation with respect to the different metal binder content for (W:Ti)C-Ni. We can see, firstly, that the porosity of the materials decreases as the Ni content increases. However, when the Ni content is high, the Ni metal binder prevents the coalescence of the carbide particles, producing a more uniform and finer grain structure. In other words, all the carbide grains are

separated by a layer of the nickel metal binder and consequently produce a normal grain growth [20-23].

The results of the high resolution SEM and the composition analysis (EDAX), as shown in Fig.6, clearly reveal that the (W:Ti)C particles have a rounded morphology with a carbide core/rim structure. This morphology is formed when the carbide particles are dissolved in the Ni liquid and re-precipitated on the large carbide grains, where they cause grain coarsening, called Ostwald ripening [24,25].

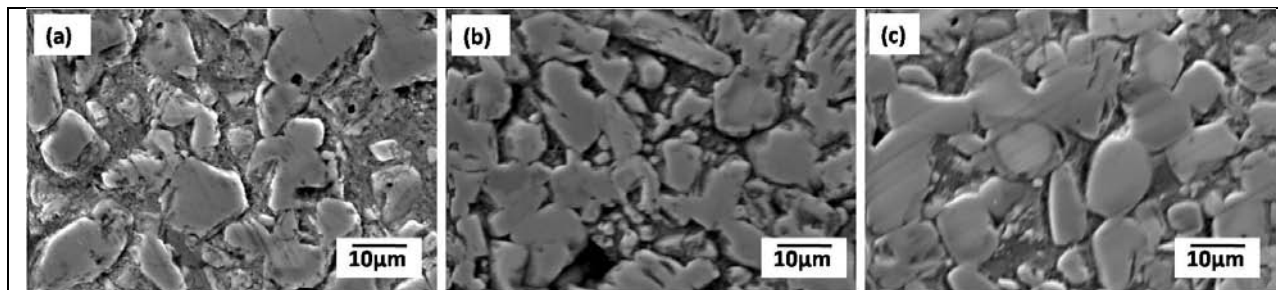


Figure 5: SEM micrographs of the cross-sectional (W:Ti)C-Ni cemented carbides samples sintered at 1450°C, where; for (a) (W:Ti)C-10 wt%Ni, (b) (W:Ti)C-20 wt%Ni, and (c) (W:Ti)C-30 wt%Ni.

According to the EDAX analysis, the estimated chemical composition of the (W:Ti)C-Ni cemented carbides, which is shown in Fig.6c which is the carbide rim, (W:Ti)C-Ni has an estimated chemical composition of  $(W_{25.67}Ti_{40.6})C_{1.73}Ni_{31.00}$  with a Ti/W ratio of 1.6. As a result of the significant difference in the way the two

phases form cemented carbides. One can show from the data of the measured density as shown in Fig.7 that by increasing the Ni binder content the density of the obtained (W:Ti)C-Ni cemented carbides were increased up to 95% in case of the (W:Ti)C-30wt%Ni.



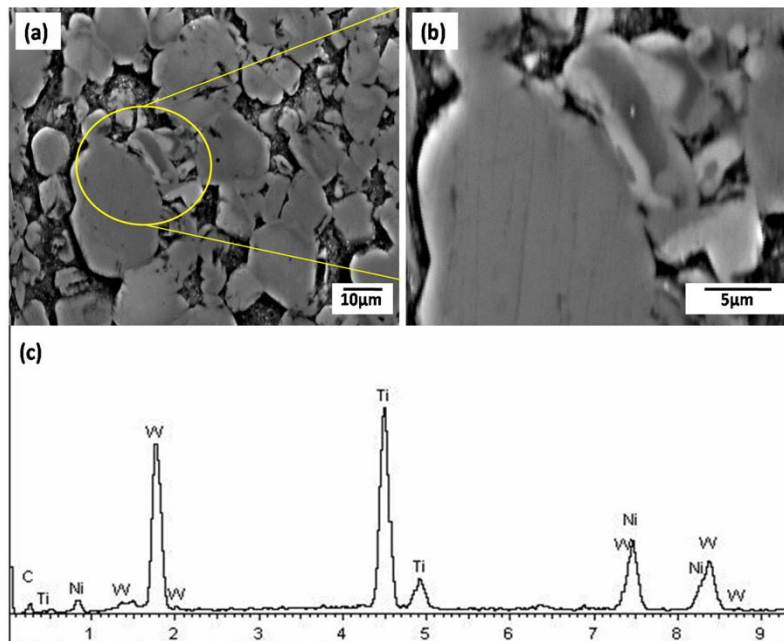


Figure 6: SEM micrographs with different magnifications and a typical compositional EDAX analysis for the cross-sectional area of the produced (W:Ti)C–30 wt. % Ni cemented carbides.

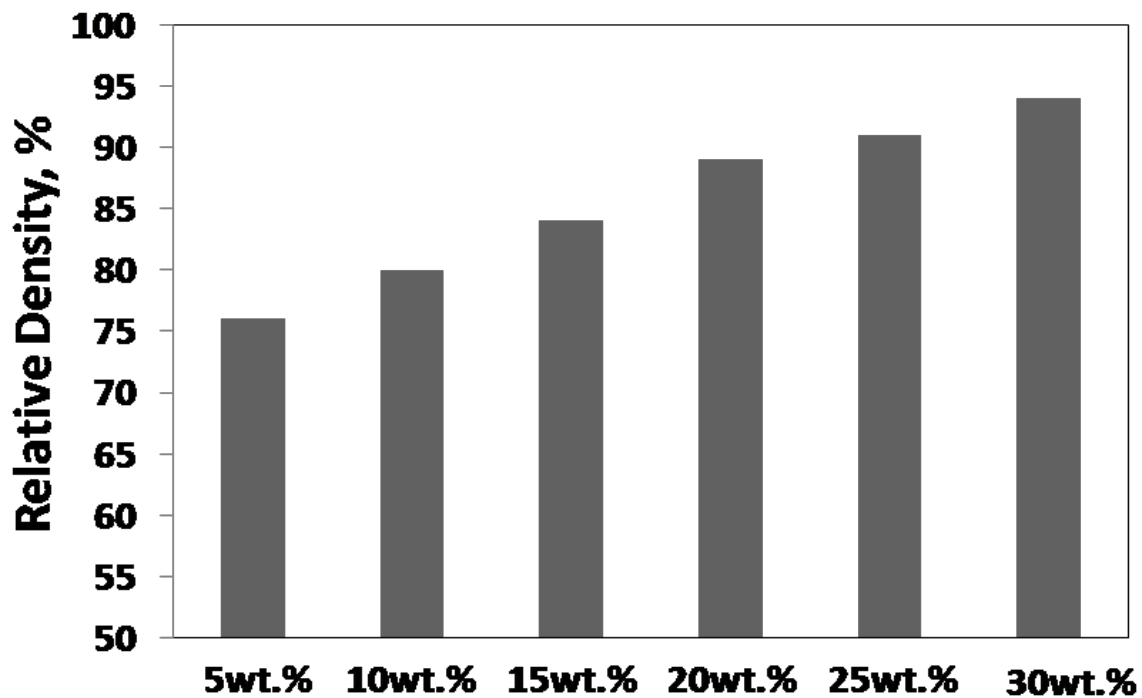


Figure 7: Effect of the Ni metal binder composition on the relative density of the produced (W:Ti)C–Ni cemented carbides by vacuum sintering at 1450°C for 1h.

Fig.8 shows the results of the measured hardness of the obtained (W:Ti)C–Ni cemented carbides indicated that the exact character of the microstructure has a critical influence on the resultant hardness. The in-situ hardness of nickel, namely 440, is much higher than the typical values of 240 for bulk nickel. This difference is

explained by the solid solution of W, Ti and C in the liquid phase binder and by the complex stress state resulting from the different thermal expansion coefficients of nickel and W, Ti and. The compositional analysis confirms that the hardening effect of nickel is due to the solid solution of Ti in the Ni binder. Moreover,

due to the solubility of WC in the TiC forming (W:Ti)C phase, the hardness value of the (W:Ti) C phase is 2530, which is higher than the micro-hardness value of the WC (1300) and lower than that of the TiC (3200). Fig. 9 also shows increasing in the hardness by increase the metal binder content. This result can be discussed due to the

densification effect. By increasing the metal binder content the porosity was decreased, the densification was increased and as a result the hardness increased and by increasing the Ni binder content which has lower hardness than the carbide phase [26].

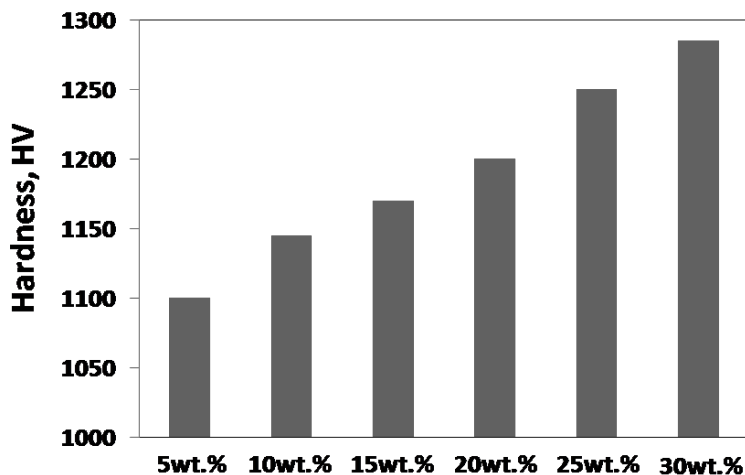


Figure 8: Effect of the Ni metal binder composition on the hardness of the produced (W:Ti)C–Ni cemented carbides by vacuum sintering at 1450°C for 1h.

The measured M–H hysteresis loops are shown in Fig. 10. The value for the mass saturation magnetization ( $M_s$ ) of the obtained (W:Ti)C–Ni series at 2 Tesla as shown in Fig. 11 is lower than the absolute saturation of 54.8 emu/g for the nickel [27]. The volume fraction of liquid phase of nickel binder affects the magnetic properties. The magnetic saturation values reveal the presence of the ferromagnetic Ni phase, which intensifies as the Ni content rises, 9 emu/g for (W:Ti)C–30wt%Ni. Three factors can contribute to the lower readings in the  $M_s$  of the obtained (W:Ti)C–Ni cemented carbides: first, the ratio of the fcc phases to the hcp phases; second, the lower saturation magnetization caused by any residual tungsten, Ti or C

that are separated or combined in a solution; and, third, the presence of carbide grains, which act as magnetic voids where opposing magnetic fields can occur and in turn reduce the saturation magnetization values [28:29]. Fig. 12 illustrates the influence of the Ni binder on the coercivity ( $H_c$ ). First, the coercivity decreases with increasing the metal binder content. Second, the sinter ability increases and the porosity decreases, thereby decreasing the particle–particle interactions and decreasing the coercivity of the materials because of the porosity values of the (W:Ti)C–Ni, and by decreasing the porosity the particle–particle interaction was decreased and the coercivity decreased [30–33].

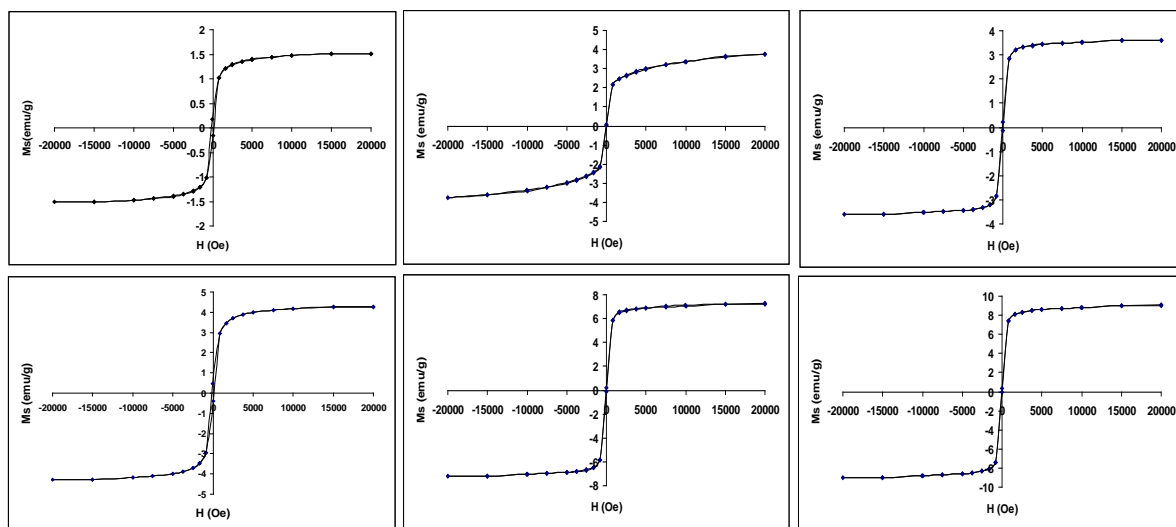


Figure 9: M–H hysteresis loops of the (W:Ti)C–Ni cemented carbides measured at 2 T for (a) (W:Ti)C–5 wt%Ni, (b) (W:Ti)C–10 wt%Ni, (c) (W:Ti)C–15 wt%Ni, (d) (W:Ti)C–20 wt%Ni, (e) (W:Ti)C–25 wt%Ni and (f) (W:Ti)C–30 wt%Ni.

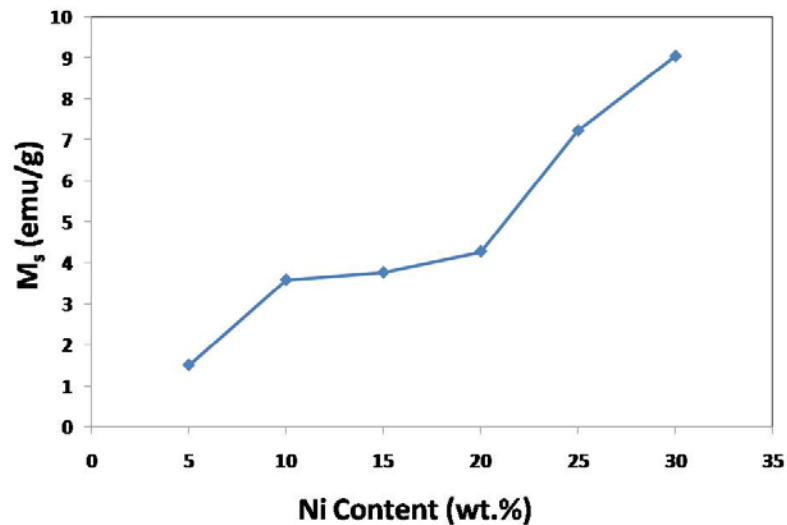


Figure 10: Effect of the Ni binder composition on the saturation induction ( $M_s$ ) of (W:Ti)C-Ni cemented carbides.

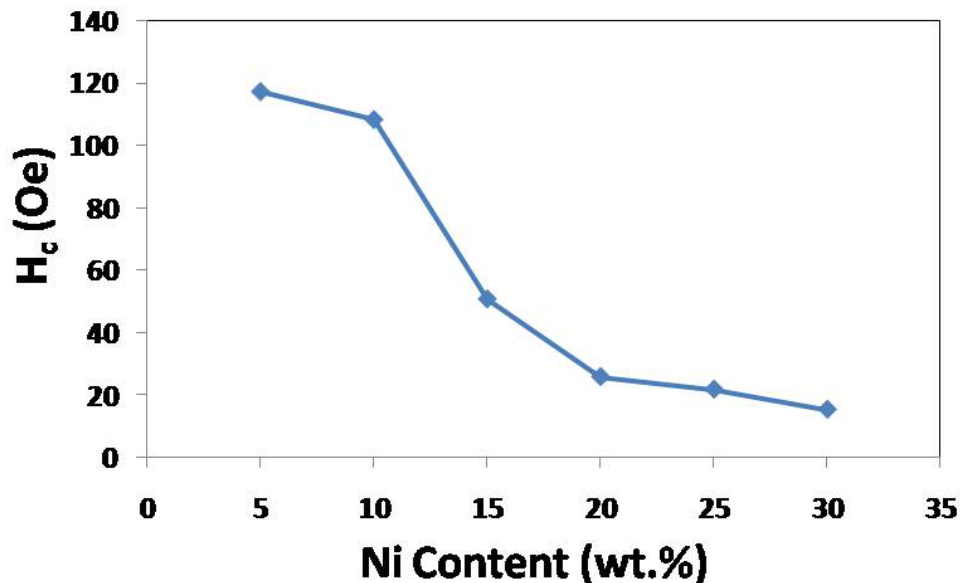


Figure 11: Effect of the Ni binder composition on the coercivity ( $H_c$ ) of (W:Ti)C-Ni cemented carbides.

#### IV. CONCLUSION

The microstructure, hardness and magnetic properties of (W,Ti)C-Ni cemented carbides were investigated. The (W:Ti)C cemented carbides were consolidated with a water atomized Ni as the liquid phase binder by using the vacuum liquid phase sintering at 1450°C. The major results are summarized as follows:

1. A pure nickel powder can be fabricated by water atomization technique. The obtained nickel powder has a fine particle size and can be used as a metal binder for the (W:Ti)C particles.
2. As the nickel binder content in the (W:Ti)C-Ni increases, the density and the hardness values increases.
3. The measured mass saturation magnetization of the (W:Ti)C-Ni cemented carbide sat 2 Tesla increases

as the Ni binder content increases, indicating the ferromagnetic nature of the materials at high field strength. As well as, the magnetic coercivity measurements indicate that the coercivity increases with increasing the porosity.

#### ACKNOWLEDGMENT

The authors wish to thank the researchers and the technicians of the Central Metallurgical R&D Institute (CMRDI) in Cairo, Egypt for their cooperation.

#### REFERENCES RÉFÉRENCES REFERENCIAS

1. Kumachiro Y. High-temperature characteristics. In: Kumashiro Y, editor. Electric refractory materials. New York-Basel: Marcel Dekker, Inc.; 2000.



2. Exner HE. Physical and chemical nature of cemented carbides. *Int. Met. Rev.* 243 (1979) 149-173.
3. Ettmayer P. Hardmetals and Cermets, *Annu. Rev. Mater. Sci.* 19 (1989) 145-164.
4. Wentzel EJ, Allen C. The erosion-corrosion resistance of tungsten-carbide *hard* metals, *Int. J. Refract. Met. Hard Mater.* 15 (1997) 81-87.
5. Imasato S, Tokumoto K, Kitada T, Sakaguchi S. Properties of ultra-fine grain binder less cemented carbide RCCFN. *Int. J. Refract. Met. Hard Mater.* 13 (5) (1995) 305-312.
6. Almond EA, Roebuck B, Identification of optimum binder phase compositions for improved WC hard metals, *Mater. Sci. Eng. A* 105/106 (1988) 237-248.
7. Gille G, Bredthauer J, Gries B, Mende B, Advanced and new grades of WC and binder powder-their properties and application, *Int. J. Refract. Met. Hard Mater.* 18 (2,3) (2000) 87-102.
8. Goeuriot P, Thereunto F, Boron as sintering assistive in cemented WC-Co(or Ni) alloys, *Ceram. Int.* 13 (2) (1987) 99-103.
9. Zhang ZG, Gesmundo F, Hou PY, Niu Y, Criteria for the formation of protective  $Al_2O_3$  scale on Fe-Al and Fe-Cr-Al alloys, *Corros. Sci.* 48(2006) 741-765.
10. Anal A, Bandyopadhyay TK, Das K., Development and characterization of ZrC-reinforced steel-based of composite, *J Mat Process Tech* 127 (2006) 70-76.
11. Jiang WH, Fei J, Han XL., In situ synthesis of (TiW)C/Fe composites, *Mater Lett.* 46 (2000) 222-224.
12. Correa EO, Alcantara NG, Tecco DG, Kumar RV, Development of an iron-based hardfacing material reinforced with Fe-(TiW)C composite powder, *Met and Mat Trans.* 38A(2007) 937-940.
13. Srivastava AK, Das K, Microstructure and abrasive wear study of (Ti,W)C-reinforced high-manganese austenitic steel matrix composite, *Materials Lett.* 62 (2008) 3947-3950.
14. Saidi A., Reaction synthesis of Fe-(W,Ti)C composites, *J Mat Process Tech.* 89-90(1999) 141-144.
15. Jung J, Kang S., Sintered (Ti,W)C carbides, *Scr Mater* 2007;56:561-4.
16. Acchar W, Cairo CA., The influence of (Ti,W)C and NbC on the mechanical behavior of Alumina, *Mater Res.* 9 (2006) 171-174.
17. Andren HO. Microstructures of cemented carbides. *Mater Design*22 (2001) 491-495.
18. Saidi A, Barati M. Production of (W,Ti)C reinforced Ni-Ti matrix composites. *J Mater Prod Technol.* 124 (2002) 166-170.
19. Engqvist H, Jacobson S, AxénN, *Wear* 252 (2002) 384.
20. Hansen M, Anderko K. Constitution of binary alloys. McGraw-Hill; 1958.
21. Burton WK, Cabrera N, Frank FC. The growth of crystals and the equilibrium structure of their surfaces. *Philos Trans Roy Soc London*243A (1951):299-304.
22. Hirth JP, Pound GM. Condensation and evaporation. Oxford: Pergamon Press; 1963. p. 77.
23. Rollett AD, Srolovitz DJ, Doherty RD, Anderson P. Computer simulation of recrystallization in non-uniformly deformed metals. *Acta Metall.* 37 (1989) 627-631.
24. Peteves SD, Abbaschian R. Growth kinetics of solid-liquid Ga interfaces. *MetallTrans A22A* (1991) 1271-1275.
25. Oh KS, Jun JY, Kim DY. Shape dependence of the coarsening behavior of niobium carbide grains dispersed in a liquid iron matrix. *J Am Ceram Soc.* 83(12) (2000) 3117-3120.
26. Andrén HO, Rolander U, Lindahl P. Phase composition in cemented carbides and cermets. *Int J Refract Met Hard Mater.* 12(1993) 107-110.
27. Daoush WM, Lee KH, Park HS, et al. Effect of liquid phase composition on the microstructure and properties of (W,Ti)C cemented carbide cutting tools. *Int J Refract Metal Hard Mater.* 27(2009) 83-89.
28. Bozorth. American institute of physics handbook5 (1957). p 206.
29. Daoush W. Ni-coated powder approach for advanced materials. PhD thesis, Faculty of science, Ein Shams University, Cairo; 2004.
30. Daoush W, Moustafa S, Kayetbay S. Processing of metallic filters by powder metallurgy technique. *Powder MetallProg.* 6(2006) 164-168.
31. Daoush W. Processing of FeCo nanosized soft-magnetic material by powder metallurgy technique. *Mater Sci Forum*558 (2007) 707-710.
32. Moustafa SF, Daoush WM. Synthesis of nanosized Fe-Ni powder by chemical process for magnetic applications. *Mater Prog Technol.* 181 (2007) 59-63.
33. Daoush W, Moustafa SF. Coating points a way for synthesis of tough intermetallics. *Met Powder Rep.* 1(2007) 30-33.